Boundary-Layer Meteorol (2011) 139:395–409
DOI 10.1007/s10546-011-9593-5

ARTICLE

# Urban Dispersion Modelling and Experiments in the Daytime and Nighttime Atmosphere

**Pasquale Franzese · Pablo Huq**

Received: 27 April 2010 / Accepted: 21 January 2011 / Published online: 19 February 2011


**Abstract** An analytical model of atmospheric dispersion in urban areas in both daytime and nighttime conditions is presented. The model is based on a Gaussian formulation where the horizontal and vertical diffusion coefficients are determined according to analytical theories. The model is validated with dispersion measurements from field experiments conducted in Oklahoma City, Salt Lake City, St. Louis and London, U.K. The theory is in good agreement with the data for both daytime and nighttime conditions. The data support the conclusion that the magnitude of the nighttime stratification in the urban atmosphere is weak; however, its effects on dispersion are not negligible. The predicted existence of two distinct dispersion regimes, in the near and in the far field, is also confirmed by the data. The good collapse of the data suggests that urban dispersion is governed by the characteristic length scales of atmospheric boundary-layer turbulence, rather than urban canopy length scales that are more likely to affect dispersion only in the vicinity of the source.

**Keywords** Atmospheric stability · Field experiments · Gaussian plume model · Urban dispersion

## 1 Introduction

Unrelenting urbanization, motorization and economic growth exacerbate already serious levels of air pollution in most urban centres (Collier 2006). The main concern is the detrimental effect of poor air quality on health (Molina and Molina 2004), but immediate consequences of air pollution are reduced visibility and odour. In addition, there is renewed concern about the safety of chemical plants from which accidental releases of materials of extreme toxicity can endanger population, and about the consequences of deliberate releases of toxic

P. Franzese (✉)
College of Science, George Mason University, Fairfax, VA 22030, USA
e-mail: pfranzes@gmu.edu

P. Huq
College of Earth, Ocean and Environment, University of Delaware, Newark, DE 19716, USA

materials in the midst of urban centres. The serious threat represented by accidental or intentional releases of chemical and biological agents is spurring increasing interest with a variety of research foci on urban micrometeorology and pollutant dispersion.

Prediction of urban air pollution dispersion is challenging because of the complex dynamics of flow over urban topography. Advances in instrumentation have led to high resolution datasets (e.g. Rotach 1995; Roth 2000; Dobre et al. 2005; Rotach et al. 2005). Comprehensive field experiments were conducted in Salt Lake City (Allwine et al. 2002), Los Angeles (Rappolt 2001), San Diego (Venkatram et al. 2002, 2004), Oklahoma City (Allwine et al. 2004) and New York City (Allwine and Flaherty 2006; Watson et al. 2006) and in simulated urban canopies at the Dugway Proving Ground (Biltoft 2001; Yee and Biltoft 2004; Milliez and Carissimo 2007, 2008). These studies provide the meteorological observations and tracer concentrations necessary to develop atmospheric models and parametrizations.

The mean concentration field of the contaminant at ground level and the chemical hazard criteria need to be known in order to conduct air pollution risk assessments (e.g. Arnot et al. 2006). The consensus for urban areas is that the maximum ground-level mean concentration $C$ as a function of the alongwind distance from the source $x$ decays according to a $C \propto x^{-2}$ power law. Robins and Cheng (2003) present an empirical relationship for an upper bound to the observed concentrations of the form:

$$\frac{CU}{Q} = \frac{K_D}{x^2} \tag{1}$$

where $U$ is the mean wind speed at building height, $Q$ is the mass release rate and the constant $K_D = 25$. This value defines an upper bound trend line below which (almost) all data points are located.

The analytical dispersion model proposed by Venkatram et al. (2005) also predicts $C \propto x^{-2}$ in field studies of dispersion at a site with buildings only one or two storeys high in Barrio Logan, San Diego, U.S.A. Hanna et al. (2007) used Eq. 1 to fit the data for the evolution of concentration with distance from the field studies at Oklahoma City (JU2003) and Salt Lake City (URBAN 2000) in the U.S.A. and London, U.K. (DAPPLE). The value of $K_D$ defining the best fit (rather than the upper bound) varied with the location and time of day. Best fits to the nighttime data were obtained using $K_D = 10$, while daytime data yielded $K_D = 3$. In other words, the scaled concentration data show a marked difference of about a factor of three or four between day and night releases. Also, a $x^{-2}$ power law may not represent the data at large distances (e.g. Fig. 6b in Hanna et al. 2007).

While it is tempting to attribute the difference between daytime and nighttime concentration data to stratification, the effects of stability on dispersion in the urban environment are relatively unexplored. It is well known that stratification strongly inhibits plume vertical dispersion in open terrain. The question whether, or to what extent, stratification exists in densely built-up areas is more controversial. Ambient stratification may be weakened by the enhanced mechanical generation of turbulence over complex geometry, and by the urban heat island, which in some cases can lead to "an almost complete absence of stable conditions" (Morrison and Webster 2005).

This article includes three main contributions:

(i) We present a Gaussian plume dispersion model, where the horizontal diffusion coefficient is determined by the theory of Taylor (1921), and the vertical diffusion coefficient by the theory of Hunt and Weber (1979). The model accounts for the observed differences between experimental data in the nighttime and daytime atmosphere, as well as the different trends for short and large distances (i.e. near and far fields).

The predictions are in good agreement with the observations from several urban dispersion experiments.

(ii) The time and length scales governing urban dispersion in the near and far fields are identified. Non-dimensionalization results in a good collapse of the data, thus defining a general framework for urban dispersion analysis and prediction.

(iii) The results show that, although stratification is weak, its effects on dispersion are not negligible.

In Sect. 2, we present the dispersion model and the derivation of the horizontal and vertical dispersion coefficients. The field experiments that will be used for analysis and comparison are summarized in Sect. 3. The results of the model comparisons with the field data are presented in Sect. 4, where the problem is also set in non-dimensional form, and statistical robustness tests are performed to quantify possible spurious correlations. Conclusions and a discussion of the results are reported in Sect. 5.

## 2 Dispersion Model

We assume that the ground-level mean concentration field $c$ of a tracer emitted from a continuous source can be approximated by a reflected Gaussian plume model, which for ground-level releases takes the form

$$c = \frac{Q}{\pi U \sigma_y \sigma_z} \exp\left(-\frac{y^2}{2\sigma_y^2}\right) \tag{2}$$

where $y$ indicates the crosswind direction and the source is located at $y = 0$, $\sigma_y$ and $\sigma_z$ are the standard deviations of the crosswind and vertical distributions of concentration, respectively, and $U$ is the mean wind speed across the plume.

### 2.1 Horizontal Dispersion

If the turbulence is assumed to be stationary and statistically homogeneous in the horizontal direction, $\sigma_y$ can be calculated according to the theory of Taylor (1921) as

$$\sigma_y^2 = \sigma_{yo}^2 + 2\sigma_v^2 \int_0^t (t-\tau) R_v(\tau) d\tau \tag{3}$$

where $\sigma_{yo}$ is the plume crosswind standard deviation at the source, $\sigma_v^2 = \langle v^2 \rangle$ is the variance of the Lagrangian crosswind velocity $v$, and $R_v(\tau) = \langle v(t)v(t+\tau) \rangle / \sigma_v^2$ is the autocorrelation coefficient of $v$. The velocity autocorrelation has been often assumed to be exponentially decaying, in the form of $R_v(\tau) = \exp(-\tau/T_y)$, where $T_y$ is the horizontal decorrelation time scale (Neumann 1978; Tennekes 1979). Substituting in Eq. 3 yields:

$$\sigma_y^2 = \sigma_{yo}^2 + 2\sigma_v^2 T_y^2 \left[\frac{t}{T_y} + \exp\left(-\frac{t}{T_y}\right) - 1\right]. \tag{4}$$

### 2.2 Vertical Dispersion

In neutral (or near-neutral) conditions the turbulent fluctuations and the friction velocity can be considered constant with height, and similarity theory can be applied in the surface layer.

We assume that the daytime atmosphere in urban areas is neutral. For the nighttime atmosphere we estimate that stratification is sufficiently weak (Roth 2000; Luhar et al. 2006) so that similarity theory also applies.

Crosswind dispersion was calculated assuming horizontally homogeneous turbulence. In the vertical direction, the presence of the ground destroys the homogeneity of the turbulence, and affects the near-ground distribution of local turbulent length scales. As a consequence, turbulence in the vertical direction cannot be considered homogeneous.

Under these conditions, $\sigma_z$ can be described by the theory of Hunt and Weber (1979), which was developed to model dispersion from ground-level sources in a neutral atmosphere. The relevant aspects of the theory are briefly summarized below. The rate of growth of $\sigma_z$ can be expressed as

$$\frac{d\sigma_z^2}{dt} = 2\int_0^t \langle w(t)w(\tau)\rangle \, d\tau \tag{5}$$

where $w$ is the Lagrangian vertical velocity. To solve Eq. 5, $w$ is decomposed into mean and fluctuating components, i.e. $w = \langle w\rangle + w'$:

$$\frac{d\sigma_z^2}{dt} = 2\,\langle w(t)\rangle \int_0^t \langle w(\tau)\rangle \, d\tau + 2\sigma_{w'}^2 \int_{-t}^0 R_{w'}(t,\tau)d\tau \tag{6}$$

where $\sigma_{w'}$ is the standard deviation of $w'$, and $R_{w'}(t,\tau) = \left\langle w'(t)w'(t+\tau)\right\rangle / \sigma_{w'}^2$.

A Lagrangian integral time scale is defined as $T_L = \int_0^\infty R_{w'}(t,\tau)d\tau \approx \int_{-t}^0 R_{w'}(t,\tau)d\tau$, and it is assumed that $T_L \propto L_{x,w}/\sigma_w$, where $L_{x,w}$ is the alongwind integral length scale for the Eulerian vertical velocity evaluated at the centre of the plume $\langle z\rangle$ (Corrsin 1963). In the surface layer $L_{x,w} \propto \langle z\rangle$ (Pasquill 1974, p. 57), and for a ground-level source $\langle z\rangle = \langle w\rangle\, t$, so one obtains $T_L \propto \langle w\rangle\, t/\sigma_w$. Lagrangian similarity theory prescribes $\sigma_w \propto u_*$, where $u_*$ is the friction velocity, and $\langle w\rangle \propto u_*$ for a ground-level source (Monin and Yaglom 1971, p. 562). As a consequence, $T_L \propto t$. Finally, because $\sigma_{w'} \propto u_*$, Eq. 6 provides (Hunt and Weber 1979):

$$\sigma_z^2 = \sigma_{zo}^2 + b^2\sigma_w^2 t^2 \tag{7}$$

where $\sigma_{zo}$ is the plume vertical standard deviation at the source, and $b$ is an empirical constant. The values $b = 1$ for a daytime atmosphere and $b = 0.5$ for a nighttime atmosphere, provided a good fit to the experimental data described in Sect. 3.

Vertical dispersion is confined to the boundary-layer height, or the height of any capping inversion. We account for the effect of such a boundary at $z = L_z$ by considering the asymptotic limit of Eq. 2 at large distance from the source, where the vertical distribution of concentration is approximately uniform. In this case, the distribution of mean concentration is described by

$$\lim_{t\to\infty} c = \frac{Q}{\sqrt{2\pi}U\sigma_y L_z}\exp\left(-\frac{y^2}{2\sigma_y^2}\right). \tag{8}$$

Comparing Eq. 8 with Eq. 2 we obtain

$$\lim_{t\to\infty} \sigma_z^2 = 2L_z^2/\pi \tag{9}$$

and hence we modify Eq. 7 to include the asymptotic limit (9) as

$$\sigma_z^2 = \sigma_{zo}^2 + \frac{b^2\sigma_w^2 t^2}{1 + b^2\sigma_w^2 t^2 \pi / 2L_z^2} \tag{10}$$

### 2.3 Asymptotic Behaviour of the Concentration Field

Both $\sigma_y$ and $\sigma_z$ admit asymptotic limits depending on the distance from the source. For travel times smaller than $T_y$, horizontal dispersion is mainly controlled by the action of the eddies larger than the dimension of the plume. The large eddies move the plume bodily causing meandering of the centreline. In this regime, i.e. for $\sigma_{yo}/\sigma_v \ll t \ll T_y$, Eq. 3 simplifies to $\sigma_y^2 = \sigma_v^2 t^2$. At larger travel times the horizontal scale of the plume becomes larger than the turbulence length scale. Therefore, at this stage the plume expands only under the action of internal eddies. The expansion in this regime is described by Eq. 3 when $t \gg T_y$, which provides $\sigma_y^2 = 2\sigma_v^2 T_y t$. The linear growth of $\sigma_y^2$ with time corresponds to a diffusive regime.

In contrast, $\sigma_z$ simply grows linearly with time till it reaches the upper boundary, at which point it becomes constant; for small travel times ($\sigma_{zo}/\sigma_w \ll t \ll T_z$), Eq. 10 yields $\sigma_z = b\sigma_w t$, and when $t \gg T_z$, Eq. 10 reduces to $\sigma_z = \sqrt{2/\pi} L_z$.

Substituting the asymptotic expressions for $\sigma_y$ and $\sigma_z$ in Eq. 2, and using the transformation $t = x/U$, we obtain the following asymptotic formulae for the maximum ground-level mean concentration $C$ at the centreline of the plume:

$$C = \left(\frac{QU}{b\pi\sigma_v\sigma_w}\right) x^{-2} \quad \text{for } x \ll UT_z \tag{11}$$

$$C = \left(\frac{Q}{2\sigma_v L_z \sqrt{\pi U T_y}}\right) x^{-1/2} \quad \text{for } x \gg UT_y \tag{12}$$

To summarize, in the near field $\sigma_y \propto x$ and $\sigma_z \propto x$; therefore Eq. 2 yields $C \propto x^{-2}$. In the far field $\sigma_y \propto x^{1/2}$, $\sigma_z = \text{const.}$ and as a consequence Eq. 2 yields $C \propto x^{-1/2}$.

## 3 Overview of the Experiments

The model will be tested by comparison with field measurements. The concentration and meteorological data that we utilize were collected during four urban experiments. A brief description of the experiments is provided below, together with information on the relevant variables $\sigma_v$, $\sigma_w$, and mean wind speed at the canopy height $U$. The similarity relationships for a neutral atmosphere within and above the urban canopy imply that the turbulent velocity fluctuations $\sigma_v$ and $\sigma_w$ are constant with height (e.g. Delle Monache et al. 2009).

### 3.1 Oklahoma City (JU2003)

The Oklahoma City urban experiment (JU2003) was conducted in June and July, 2003, and consisted of 10 Intensive Operating Periods (IOP) of 8 h each, where sulphur hexafluoride ($SF_6$) was released from one of three near-ground release locations. IOPs 01 through 06 were conducted during daytime, IOPs 07 through 10 during the night. In accord with Hanna et al. (2007), nighttime atmosphere was assumed for IOP05 trials 1 and 2 because they were conducted in the early morning and because low mixing depths were observed. The releases were either continuous with a duration of 30 min, or instantaneous, which are not considered

in this study. During each IOP, three consecutive releases were made at 2-h intervals. Concentration samplers were located at distances ranging from about 200 m to 4 km. In this study we use the 30-min averaged maximum concentrations $C$, wind speeds $U$, and turbulence measurements of $\sigma_v$ and $\sigma_w$ which are reported by Hanna et al. (2007). An overview of the JU2003 experiments is presented in Allwine et al. (2004), a comprehensive description and technical details are given in Clawson et al. (2005). The experimental dataset for JU2003 is digitally archived at Dugway Proving Ground (2005).

### 3.2 Salt Lake City (URBAN 2000)

The urban dispersion field experiments in Salt Lake City (URBAN 2000) were conducted in September and October, 2000 (Allwine et al. 2002). The releases consisted of 1-h nighttime constant rate emissions of $SF_6$ from a near ground-level point source or a 30 m line source. Samplers measuring 30-min average concentrations were located at distances ranging from 150 m up to 6 km from the source. Detailed concentration and wind observations are reported in Hanna et al. (2003). The data are available for six IOPs, each consisting of three consecutive releases. As described by Hanna et al. (2003), IOPs 02, 04, 05 and 07 were conducted under consistently very low wind speeds, averaging about $0.5\,\mathrm{m\,s^{-1}}$ at building level, whereas moderate winds averaging about $1\,\mathrm{m\,s^{-1}}$ at building level were recorded during IOP 09 and 10. Accordingly, we assumed nighttime atmospheric conditions for IOPs 02, 04, 05 and 07, and daytime conditions for IOP 09 and 10. The advection velocity $U$ for each trial was assumed equal to the wind speed values which were obtained averaging the building-level observations reported in Hanna et al. (2003) (i.e. two "D" and four "M" anemometers). The velocity standard deviations $\sigma_v$ and $\sigma_w$ were estimated for all experiments using the empirical formulae $\sigma_v = 0.5u_c$ and $\sigma_w = 0.33u_c$ proposed by Hanna et al. (2007), where $u_c$ is a characteristic wind speed within the canopy. We calculated $u_c$ by averaging all building-level and ground-level observations for all trials.

### 3.3 London (DAPPLE)

The DAPPLE (Dispersion of Air Pollution and its Penetration into the Local Environment) project is a multi-year experimental campaign conducted in London, U.K. since 2002 (DAPPLE 2002). We analyse the data from the first tracer study, which took place between April 28 and May 23, 2003. Perfluorocarbon (PFC) tracer was released by a near-ground source for a duration of 15 min, and detected by ten samplers located at distances from 75 up to 430 m from the source, measuring ten consecutive 3-min average concentrations. Data from nine samplers are available, all but one located at ground level. We use the source release rate, receptor distances, wind speeds and maximum 3-min average concentrations reported by Neophytou and Britter (2004), who assumed $U = 3\,\mathrm{m\,s^{-1}}$ for all trials, corresponding to the mean wind speed measured by a single instrument at a height of 30 m, and estimated the in-canopy wind speed as $u_c = 2.168\,\mathrm{m\,s^{-1}}$. Turbulent fluctuations were estimated as $\sigma_v = 0.5u_c$ and $\sigma_w = 0.33u_c$ (Hanna et al. 2007).

### 3.4 Saint Louis

The St. Louis dispersion study (McElroy and Pooler 1968) consisted of 26 daytime and 16 evening experiments, which were conducted in seven series between May 1963 and March 1965. Fluorescent zinc cadmium sulphide (ZnCdS) particles were released for about 1 h from

one of two sources located near the ground. Dosage at the surface was measured by samplers located along circular arcs at distances between about 600 m and 16 km. The present analysis includes data from the daytime experiments conducted in neutral conditions (i.e. Pasquill's stability class D) and the evening experiments conducted in stable conditions (stability class F).

For the daytime cases, we estimated $U$ at building-level $H$ using a log profile for the wind speed $u(z)$:

$$u(z) = \frac{u_*}{\kappa} \log\left(\frac{z-d}{z_o}\right) \tag{13}$$

where the von Karman constant $\kappa = 0.4$, a mean building height $H = 20$ m was assumed, and we estimated the displacement height $d = 0.5H$ and roughness length $z_o = 0.15H$ as recommended by Hanna et al. (2003). The friction velocity $u_*$ was calculated from Eq. 13 using the mean of the observed 'effective transport wind speed' $u_e$ at a height of 140 m. For most daytime experiments, $u_e$ was obtained from mean tethered meteorological balloon trajectories and was found to be in good agreement with the wind speed measurements at the 140 m level of a tower (McElroy and Pooler 1968).

Roth's (2000) comprehensive review of atmospheric turbulence data over cities shows that the similarity relationships commonly used for open terrain also apply to urban terrain above the roughness sub-layer. A similar result was found by Hanna et al. (2007) in Oklahoma City. In accordance with Roth (2000), turbulent fluctuations were estimated as $\sigma_v = 1.9u_*$ and $\sigma_w = 1.3u_*$.

For each experiment in nighttime conditions, empirical power law profiles of the wind are available in the original report. For the nighttime cases, $U$ was calculated as the average at $H$ of the reported power law profiles, and the turbulent fluctuations were calculated as $\sigma_v = 0.5u_c$ and $\sigma_w = 0.33u_c$, where $u_c$ was estimated as $u_c = U/3$ (Hanna et al. 2007).

## 4 Data Analysis and Comparison with Model Predictions

In the immediate vicinity of the source the flow field is dominated by the effects of individual buildings, and the predictions of a simple model cannot be expected to be accurate. It is difficult to rigorously establish a minimum distance for the applicability of the model. The closest concentration measurement was recorded in the DAPPLE experiment, by samplers located at 75 m from the source. At that distance, the horizontal and vertical spreads are comparable to the building scales. The model is less and less accurate at shorter distances.

At the range of distances considered in this study (up to 16 km), the buildings of the urban canopy can be considered as roughness elements, and dispersion is governed by the above-canopy turbulence scales. The horizontal and vertical turbulence time scales were estimated as $T_y = L_y/\sigma_v$ and $T_z = L_z/\sigma_w$, respectively, where $L_y$ is the horizontal turbulence length scale, and $L_z$ is the vertical turbulence length scale, which is assumed to equal the height of the boundary layer or the capping inversion.

The depth of the boundary layer is site-specific, and varies with the time of the day or night. Typical values are reported in several studies (see Stull 1988; Garratt 1992). Broadly, in a stable atmosphere the boundary-layer depth ranges from about 100 to about 300 m. We assume as a typical depth in nighttime conditions $L_z = 200$ m. In convective conditions the boundary-layer depth ranges from about 1,000 to about 2,000 m. For the neutral boundary layer we assume $L_z = 800$ m, i.e. below the lower bound of a convective boundary layer.

**Table 1** Estimates of turbulence and flow characteristics in the experiments

| Experiment | Stability | $\overline{U}$ (m s$^{-1}$) | $L_y$ (m) | $L_z$ (m) | $\sigma_v$ (m s$^{-1}$) | $\sigma_w$ (m s$^{-1}$) | $T_y$ (s) | $T_z$ (s) |
|---|---|---|---|---|---|---|---|---|
| Salt Lake City | Daytime | 1.03 | 2,000 | 800 | 0.52 | 0.34 | 3,883 | 2,354 |
| | Nighttime | 0.49 | 1,000 | 200 | 0.25 | 0.16 | 4,082 | 1,237 |
| Oklahoma City | Daytime | 2.13 | 2,000 | 800 | 1.09 | 0.70 | 1,835 | 1,143 |
| | Nighttime | 2.08 | 1,000 | 200 | 0.99 | 0.68 | 1,010 | 294 |
| St. Louis | Daytime | 2.79 | 2,000 | 800 | 1.76 | 1.20 | 1,137 | 665 |
| | Nighttime | 2.72 | 1,000 | 200 | 0.45 | 0.30 | 2,208 | 669 |
| London | Daytime | 3.00 | 2,000 | 800 | 1.08 | 0.72 | 1,845 | 1,118 |

$\overline{U}$ is the advection velocity averaged over all trials of each experiment, $L_y$ and $L_z$ are the horizontal and vertical atmospheric turbulence length scales, $\sigma_v$ and $\sigma_w$ are the crosswind and vertical velocity fluctuations, and $T_y$ and $T_z$ are the horizontal and vertical atmospheric turbulence time scales

The magnitude of $L_y$ is comparable to the wavelength $\lambda_v$ associated with the peak frequency of the energy spectral density of the crosswind velocity. Velocity spectra from several urban experiments are reported by Roth (2000). For neutral atmosphere, the wavelengths of the spectral peak are $\lambda_v \approx (30\text{–}60)H$ at a height of $6H$, where $H$ is the mean building height (Roth 2000). The values of $\lambda_v$ from the urban experiments are in good agreement with the rural observations from the Kansas experiment (Kaimal et al. 1972), which grow approximately linearly with height as $\lambda_v \approx z/0.22$ (Kaimal and Finnigan 1994; Roth 2000). Since in our cases $H \approx 20$ m, for a neutral boundary layer $\lambda_v$ ranges from about 500 m (at $6H$) to about 3,600 m (at a height of 800 m). We use $L_y = 2{,}000$ m for daytime conditions.

For a stable boundary layer the available data in Roth (2000), which only extend to a height of $3H$, show that the values of $\lambda_v$ are comparable to those in a neutral boundary layer. Assuming a similar trend with height as for the neutral case, $\lambda_v$ ranges from about 400 m (at a height of $3H$) to about 1,400 m (at a height of 300 m). We use $L_y = 1{,}000$ m as a typical value for nighttime conditions.

Table 1 reports the estimated $L_y$ and $L_z$, $\sigma_v$ and $\sigma_w$, $T_y$ and $T_z$, and the average advection velocity $\overline{U}$ for each experiment. Because the variables in our model are ensemble averages, a general requirement for a meaningful comparison is that the averaging time of the observations should be larger than the Eulerian correlation time scale. The typical averaging time for the concentration measurements in the experiments is 30 min. The Eulerian time scale can be represented by $T_y$, which ranges from 15 to 60 min. While the averaging time may not be larger than the Eulerian time scale, it is of the same order of magnitude and the errors are expected to be small. The case of the DAPPLE experiment differs, as the release was for a shorter duration, (i.e. 15 min). The concentration was collected in three-minute bins for 30 min. Neophytou and Britter (2004) noted that a constant concentration was not apparent in the concentration records for the DAPPLE data, presumably because of the short duration of the release; therefore, they used the maximum three-minute averaged concentration as representative of a continuous release. The same maximum three-minute averaged data were used in Hanna et al. (2007), and in this study.

Figure 1 shows the scaled maximum concentration $C/Q$ at ground level (in s m$^{-3} \times 10^6$) predicted by Eq. 2 versus the corresponding observations for all experiments. The data from the nighttime experiments are reported in the left panel, the daytime experiments in the central panel, and all data combined are reported in the right panel. The nighttime observations include 121 data points spanning over about three decades of concentration values, the daytime observations include 102 data points spanning about four decades of concentration

**Table 2** Statistical measures of error between modelled and observed scaled concentrations $C/Q$

| | Corr | FB | NMSE | VG | Fac2 |
|---|---|---|---|---|---|
| Nighttime | 0.83 | 0.34 | 1.62 | 1.92 | 63.64 |
| Daytime | 0.84 | 0.50 | 2.19 | 1.82 | 64.71 |
| All data | 0.73 | 0.07 | 1.78 | 1.87 | 64.13 |

The table includes correlation (Corr), fractional bias (FB), normalized mean square error (NMSE), geometric variance (VG), and the percentage of predictions falling within a factor two of the observations (Fac2)

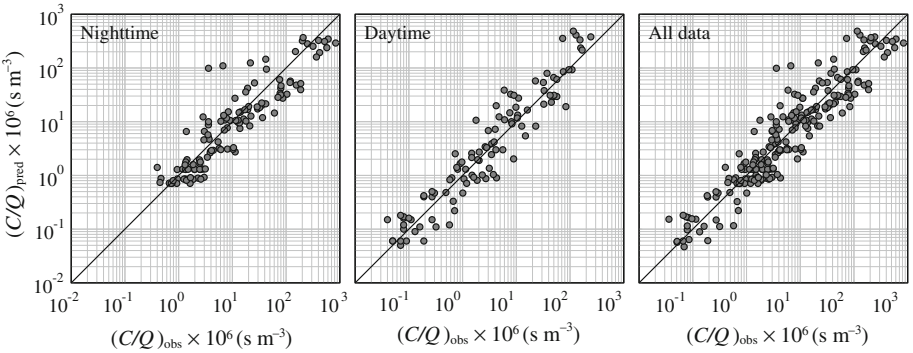


**Fig. 1** Predicted versus observed scaled concentration $C/Q$: nighttime experiments (*left panel*), daytime experiments (*centre panel*), and all data combined (*right panel*)

values. The accuracy of the predictions can be assessed by several performance statistics, which are commonly used to evaluate dispersion models (e.g. Chang and Hanna 2004). We calculated the correlation (Corr), fractional bias (FB), normalized mean square error (NMSE), geometric variance (VG), and the percentage of predictions falling within a factor two of the observations (Fac2). Table 2 reports their values for nighttime experiments, daytime experiments, and all data combined. All measures indicate a good agreement between modelled and observed concentrations.

Further insight can be derived considering non-dimensional variables. Following Davidson et al. (1995, 1996) the concentration experimental data were non-dimensionalized as $CUL_yL_z/Q$, where $U$ is the advection velocity for each observation. The distance from the source $x$, at which the observations were made, was non-dimensionalized as $x/UT$, where $T = \sqrt{T_yT_z}$.

In order to transform Eq. 2 into a non-dimensional equation, the relationship $t = x/U$ was used, and $T_y$ and $T_z$ were derived as functions of $T$ as follows:

$$T_y = \sqrt{\frac{L_y\sigma_w}{L_z\sigma_v}}\,T, \tag{14a}$$

$$T_z = \sqrt{\frac{L_z\sigma_v}{L_y\sigma_w}}\,T. \tag{14b}$$

In our calculations, the relationship $\sigma_v/\sigma_w \approx 0.5/0.33$ was used in Eqs. 14a and 14b. A finite source size corresponding to $\sigma_{yo} = \sigma_{zo} = 3\,\mathrm{m}$ was used in Eqs. 4 and 10. However,

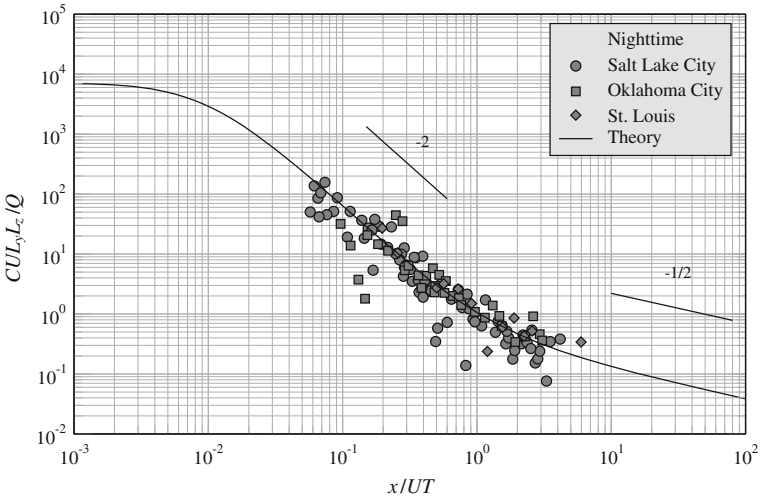


**Fig. 2** Observed non-dimensional concentration data from the experiments reported in the legend as functions of the non-dimensional distance from the source for nighttime conditions, along with the theoretical prediction, Eq. 2. The *straight lines* are proportional to $(x/UT)^{-2}$ and $(x/UT)^{-1/2}$

because the source size affects the modelled concentration only at short distances from the source, its effects are practically negligible at the large distances considered in our analysis. If the present modelling framework is applied to simulate near-source dispersion, a larger virtual source size may need to be used to account for the enhanced initial dispersion caused by the presence of surrounding building obstacles.

Figure 2 shows the non-dimensional concentration $CUL_yL_z/Q$ as a function of the non-dimensional distance $x/UT$ for the experiments conducted in nighttime conditions, along with the analytical prediction given by Eq. 2. The nighttime data points, spanning over about three decades of non-dimensional concentration values, were collected over distances from the source ranging about two orders of magnitudes. Figure 3 shows the data along with Eq. 2 for daytime conditions. The daytime data span about four decades of non-dimensional concentration values, and about three decades of distances.

In Figs. 2 and 3, the non-dimensional concentration approaches a constant value as $x$ tends to zero. This is due to the finite source size used in the equations. The predicted slope $x^{-2}$ in the near field and $x^{-1/2}$ in the far field are also shown in the figures. The data support the existence of both regimes, although it would be desirable to obtain more data in the far field, e.g. for $x > 10UT$.

The change of slope from $x^{-2}$ to $x^{-1/2}$ displayed by the theoretical curve at large distance is very gradual because the changes of slope of $\sigma_y$ and of $\sigma_z$ occur at different times. Equation 4 shows that $\sigma_y$ changes its slope from $\sigma_y \propto x^1$ to $\sigma_y \propto x^{1/2}$ approximately at $t \sim 2T_y$, whereas Eq. 10 shows that the change of slope of $\sigma_z$ from $\sigma_z \propto x^1$ to $\sigma_z \propto x^0$ occurs approximately at $t \sim 2T_z/\pi b$.

Asymptotic values of concentration can be determined from Eqs. 11, 12, 14a and 14b:

$$\frac{CUL_yL_z}{Q} = \frac{1}{\pi b}\left(\frac{x}{UT}\right)^{-2} \quad \text{for } x \ll UT \tag{15}$$

$$\frac{CUL_yL_z}{Q} = \sqrt{\frac{T}{4\pi T_z}}\left(\frac{x}{UT}\right)^{-1/2} \quad \text{for } x \gg UT \tag{16}$$

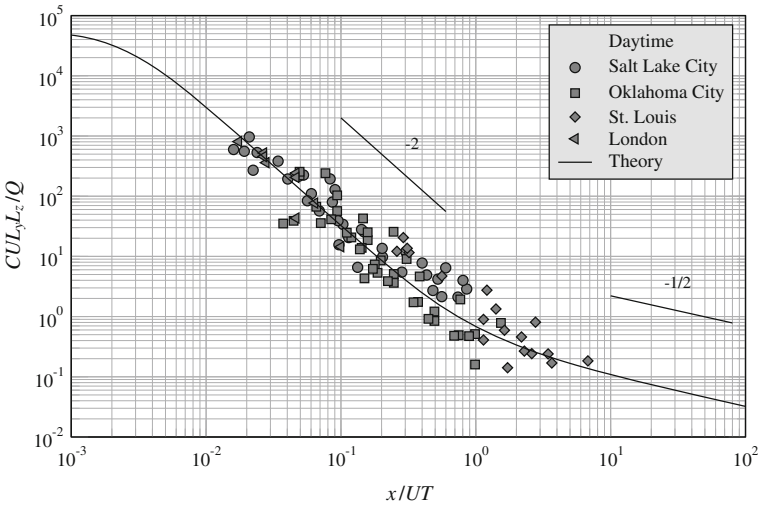


**Fig. 3** Observed non-dimensional concentration data from the experiments reported in the legend as functions of the non-dimensional distance from the source for daytime conditions, along with the theoretical prediction, Eq. 2. The *straight lines* are proportional to $(x/UT)^{-2}$ and $(x/UT)^{-1/2}$

**Table 3** Statistical measures of error between modelled and observed non-dimensional concentrations $CUL_yL_z/Q$

| | Corr | FB | NMSE | VG | Fac2 |
|---|---|---|---|---|---|
| Nighttime | 0.83 | 0.29 | 1.41 | 1.65 | 79.34 |
| Daytime | 0.91 | 0.53 | 1.58 | 2.13 | 53.92 |

Abbreviations as in Table 2

The slope coefficients in Eqs. 15 and 16 can be calculated since $T/T_z = L_y\sigma_w/L_z\sigma_v$ and $\sigma_v \approx 1.5\sigma_w$. For nighttime atmosphere, $1/\pi b = 0.64$ and $\sqrt{T/4\pi T_z} = 0.38$; for daytime atmosphere, $1/\pi b = 0.32$ and $\sqrt{T/4\pi T_z} = 0.32$.

Table 3 reports the same performance statistics listed in Table 2, but calculated for the non-dimensional variables. Table 3 also shows good agreement between model and data, suggesting that the non-dimensional variables chosen provide a relevant description of dispersion over urban canopies. Note that the non-dimensional variables do not include geometric characteristics of urban areas such as mean building height, width, spacing and area factors.

### 4.1 Spurious Self-Correlation Estimation

If two groups of variables contain one or more common variables, a certain amount of correlation amongst the compound variables may be spurious (Pearson 1897; Yule 1910; Reed 1921; Hicks 1978; Aldrich 1995). Since the variable $CUL_yL_z/Q$ can also be written as $CU\sigma_v\sigma_wT^2/Q$, the non-dimensional groups $CUL_yL_z/Q$ and $x/UT$ both include the variables $U$ and $T$, and there is the possibility that the observed relationship between the groups is partially spurious. The apparent correlation may be to a certain extent an artefact of the particular scaling used to non-dimensionalize the variables $C$ and $x$.

In order to assess the magnitude and statistical significance of the spurious component of the correlation, we performed two statistical robustness tests on the variables

**Table 4** Statistical measures characterizing the linear regressions $\log(CUL_yL_z/Q)$ vs $\log(x/UT)$ and $\log(C\sigma_v\sigma_w/Q)$ vs. $\log(x)$

| | $R^2$ | $\beta$ | $\delta$ | $t$ | $p > \|t\|$ | 95% Conf. int. | |
|---|---|---|---|---|---|---|---|
| $\log(CUL_yL_z/Q)$ vs. $\log(x/UT)$ | 0.89 | −1.57 | 0.06 | −28.30 | 0.00 | [−1.68, −1.46] | Daytime |
| $\log(C\sigma_v\sigma_w/Q)$ vs. $\log(x)$ | 0.86 | −1.58 | 0.06 | −25.17 | 0.00 | [−1.71, −1.46] | |
| $\log(CUL_yL_z/Q)$ vs. $\log(x/UT)$ | 0.85 | −1.46 | 0.06 | −25.87 | 0.00 | [−1.57, −1.35] | Nighttime |
| $\log(C\sigma_v\sigma_w/Q)$ vs. $\log(x)$ | 0.75 | −1.44 | 0.08 | −18.91 | 0.00 | [−1.59, −1.29] | |

The table includes the coefficient of determination $R^2$, the regression coefficient (or slope) $\beta$, its standard error $\delta$, the $t$-test statistic of the null hypothesis $\beta = 0$, the probability $p$ of obtaining a larger $t$ assuming $\beta = 0$, and the 95% confidence intervals for both daytime and nighttime cases

$\log(CUL_yL_z/Q)$ and $\log(x/UT)$. The logarithms are used to operate with linear relationships between the variables.

The first test is a comparison of the linear regression of $\log(CUL_yL_z/Q)$ vs. $\log(x/UT)$ with the linear regression of $\log(C\sigma_v\sigma_w/Q)$ vs. $\log(x)$ (i.e. the variables obtained after removing the common variables $U$ and $T$). Statistical measures characterizing the linear regressions are reported in Table 4. The results indicate very clearly the robustness of the correlation between $\log(C\sigma_v\sigma_w/Q)$ and $\log(x)$. The coefficient of determination $R^2$ is always above 0.75 showing a strong correlation. The high absolute values of the t-test statistic $t$ and the small 95% confidence intervals indicate rejection of the null hypothesis that the regression coefficient $\beta = 0$ in all cases. More important, all the measures are insensitive to the removal of $U$ and $T$, suggesting that their effect is likely to be irrelevant.

The impact of the common variables $U$ and $T$ on the correlation between the original compound variables can be directly assessed using a Monte Carlo bootstrapping resampling method (Efron 1981). We estimate the properties and variability of $\beta$ in the relationship $\log(CU\sigma_v\sigma_wT^2/Q)$ vs. $\log(x/UT)$ when $\log(C\sigma_v\sigma_w/Q)$ is replaced by random values (e.g. Jackson and Somers 1991; Brett 2004; Vickers et al. 2009). The set of random values of $\log(C\sigma_v\sigma_w/Q)$ is generated according to a Gaussian probability distribution with the same mean and standard deviation as the original experimental dataset. A total of 10,000 bootstrap samples has been used. Table 5 reports the values of $\beta$ in the bootstrap distribution discretized according to representative percentiles, its average $\langle\beta\rangle$ over all the bootstrap samples and its standard deviation $\sigma_\beta$. The values of $\beta$ obtained for the randomized tests are consistently small, especially in comparison with the original $\beta = -1.57$ for the daytime data and $\beta = -1.46$ for the nighttime data as reported in Table 4. This indicates a lack of correlation in the randomized data, which implies that the common variables $U$ and $T$ generate negligible correlation.

In summary, the combined results from the two tests indicate that: (i) The variables $\log(CUL_yL_z/Q)$ and $\log(x/UT)$ are strongly correlated; (ii) The correlation between $\log(CUL_yL_z/Q)$ and $\log(x/UT)$ is mainly due to the correlation between $\log(C\sigma_v\sigma_w/Q)$ and $\log(x)$; and (iii) The amount of spurious correlation introduced by the common variables $U$ and $T$ is negligible.

## 5 Discussion

We propose a model of dispersion in urban areas based on a simple Gaussian plume model, where the horizontal and vertical dispersion coefficients are determined by the theories of

**Table 5** Distribution of the regression coefficient $\beta$ in the relationship $\log(CU\sigma_v\sigma_w T^2/Q)$ vs $\log(x/UT)$ when $\log(C\sigma_v\sigma_w/Q)$ is replaced by random values using 10,000 Monte Carlo bootstrap resamples

| Percentiles | $\beta$, daytime data | | $\beta$, nighttime data | |
|---|---|---|---|---|
| | | Smallest | | Smallest |
| 1% | −0.67 | −0.86 | −0.41 | −0.57 |
| 5% | −0.57 | −0.83 | −0.30 | −0.57 |
| 10% | −0.53 | −0.82 | −0.24 | −0.56 |
| 25% | −0.44 | −0.81 | −0.15 | −0.55 |
| 50% | −0.34 | | −0.04 | |
| | | Largest | | Largest |
| 75% | −0.24 | 0.19 | 0.06 | 0.49 |
| 90% | −0.15 | 0.20 | 0.17 | 0.49 |
| 95% | −0.10 | 0.21 | 0.21 | 0.52 |
| 99% | −0.01 | 0.23 | 0.32 | 0.54 |
| $\langle\beta\rangle$ | −0.34 | | −0.04 | |
| $\sigma_\beta$ | 0.14 | | 0.16 | |

The values of $\beta$ are discretized according to a few representative percentiles. The smallest and largest $\beta$ in each bin are reported for the percentiles smaller and larger than 50%, respectively. The average over all the bootstrap samples $\langle\beta\rangle$ and standard deviation $\sigma_\beta$ are also reported

Taylor (1921) and Hunt and Weber (1979), respectively. The model applies to both daytime and nighttime conditions.

To validate the model, we have analysed field data from dispersion experiments conducted in Oklahoma City, Salt Lake City, London, and St. Louis. The data cover about four decades of concentration for the daytime cases, and about three decades for the nighttime cases. The agreement between data and theory is good for both daytime and nighttime conditions. The plots of predicted versus observed $C/Q$ show no systematic deviation, and more than 60% predictions within a factor two of the observations (Fig. 1).

The concentration data were made non-dimensional assuming that the parameters governing dispersion in the urban environment are $L_y$, $L_z$, $\sigma_v$, $\sigma_w$, and $U$. The non-dimensional concentration data for all cities collapse well, display a robust correlation, and are also in good agreement with the theory (Figs. 2, 3). The data support the predicted existence of two different dispersion regimes, the near and the far field. The results show that the effects of stratification in the urban environment are not negligible. This is indicated by the smaller value of the coefficient $b$ in Eq. 10 resulting in a smaller $\sigma_z$ for nighttime conditions.

Note that the magnitudes of $L_y$ and $L_z$ are characteristic of atmospheric turbulence, and are much larger than the building scales. Urban geometric characteristics are expected to have a more significant role only near the source. The same set of values of $L_y$ and $L_z$ were used for all four cities. We found that the results of the model are quite insensitive to large variations of $L_y$ and $L_z$. This is because in the near field, where most of the observations are located, the model is independent of $L_y$ and $L_z$ since $\sigma_y = \sigma_v t$ and $\sigma_z = b\sigma_w t$. However, the values of $L_y$ and $L_z$ determine the transition point from the near field (where $\sigma_y \propto t$ and $\sigma_z \propto t$) to the far field (where $\sigma_y \propto t^{1/2}$ and $\sigma_z = \text{const.}$) and the evolution in the far field.

**Acknowledgments** This material is partly based upon work supported by the National Science Foundation under Grant AGS 0849190 and 0849191. We thank Dr. Ugo Panizza for many enlightening discussions, and for his contributions to designing and performing the statistical robustness tests.

## References

Aldrich J (1995) Correlations genuine and spurious in Pearson and Yule. Stat Sci 10(4):364–376

Allwine KJ, Flaherty JE (2006) Urban dispersion program MSG05 field study: summary of tracer and meteorological measurements. Technical Report PNNL-15969, Pacific Northwest National Laboratory, Richland, Washington 99352

Allwine KJ, Shinn JH, Streit GE, Lawson KL, Brown M (2002) Overview of URBAN 2000: a multiscale field study of dispersion through an urban environment. Bull Am Meteorol Soc 83(4):521–536

Allwine KJ, Leach MJ, Stockham LW, Shinn JS, Hosker RP, Bowers JF, Pace JC (2004) Overview of Joint Urban 2003—an atmospheric dispersion study in Oklahoma City. In: Symposium on planning, nowcasting and forecasting in the urban zone, January 11–15, Seattle, WA. American Meteorological Society, Boston

Arnot JA, Mackay D, Webster E, Southwood JM (2006) Screening level risk assessment model for chemical fate and effects in the environment. Environ Sci Technol 40(7):2316–2323

Biltoft CA (2001) Customer report for Mock Urban Setting Test. Technical Report WDTC-FR-01-121, U.S. Army Dugway Proving Ground, Dugway, Utah

Brett MT (2004) When is a correlation between non-independent variables "spurious"? Oikos 105(3):647–656

Chang JC, Hanna SR (2004) Air quality model performance evaluation. Meteorol Atmos Phys 87:167–196

Clawson KL, Carter RG, Lacroix DJ, Biltoft CA, Hukari NF, Johnson RC, Rich JD, Beard SA, Strong T (2005) Joint Urban 2003 (JU03) $SF_6$ atmospheric tracer field tests. Technical Report, Air Resources Lab., Silver Spring, MD

Collier CG (2006) The impact of urban areas on weather. Q J Roy Meteorol Soc 132(614):1–25

Corrsin S (1963) Estimates of the relations between Eulerian and Lagrangian scales in large Reynolds number turbulence. J Atmos Sci 20:115–119

DAPPLE (2002) Dispersion of Air Pollution and its Penetration into the Local Environment. http://www.dapple.org.uk

Davidson MJ, Mylne KR, Jones CD, Phillips JC, Perkins RJ, Fung JCH, Hunt JCR (1995) Plume dispersion through large groups of obstacles—a field investigation. Atmos Environ 29:3245–3256

Davidson MJ, Snyder WH, Lawson RE, Hunt JCR (1996) Wind tunnel simulations of plume dispersion through groups of obstacles. Atmos Environ 30:3715–3731

Delle Monache L, Weil J, Simpson M, Leach MJ (2009) A new urban boundary layer and dispersion parameterization for an emergency response modeling system: tests with the Joint Urban 2003 data set. Atmos Environ 43:5807–5821

Dobre A, Arnold SJ, Smalley RJ, Boddy JWD, Barlow JF, Tomlin AS, Belcher SE (2005) Flow field measurements in the proximity of an urban intersection in London, UK. Atmos Environ 39(26):4647–4657

Dugway Proving Ground (2005) Data archive for JU2003. http://ju2003-dpg.dpg.army.mil

Efron B (1981) Nonparametric estimates of standard error: the jackknife, the bootstrap and other methods. Biometrika 68(3):589–599

Garratt JR (1992) The atmospheric boundary layer. Cambridge University Press, Cambridge, U.K., 316 pp

Hanna SR, Britter RE, Franzese P (2003) A baseline urban dispersion model evaluated with Salt Lake City and Los Angeles tracer data. Atmos Environ 37(36):5069–5082

Hanna SR, White J, Zhou Y (2007) Observed winds, turbulence, and dispersion in built-up downtown areas of Oklahoma City and Manhattan. Boundary-Layer Meteorol 125(3):441–468

Hicks BB (1978) Some limitations of dimensional analysis and power laws. Boundary-Layer Meteorol 14:567–569

Hunt JCR, Weber AH (1979) A Lagrangian statistical analysis of diffusion from a ground-level source in a turbulent boundary layer. Q J Roy Meteorol Soc 105(444):423–443

Jackson DA, Somers KM (1991) The spectre of 'spurious' correlations. Oecologia 86(1):147–151

Kaimal JC, Finnigan JJ (1994) Atmospheric boundary layer flows: their structure and measurement. Oxford University Press, New York, 289 pp

Kaimal JC, Wyngaard JC, Izumi Y, Coté OR (1972) Spectral characteristics of surface-layer turbulence. Q J Roy Meteorol Soc 98(417):563–589

Luhar AK, Venkatram A, Lee SM (2006) On relationships between urban and rural near-surface meteorology for diffusion applications. Atmos Environ 40(34):6541–6553

McElroy JL, Pooler F (1968) The St. Louis dispersion study, vol II—analysis. Technical Report Pub. No. AP-53, National Air Pollution Control Administration, US Department of Health, Education, and Welfare, Durham, NC

Milliez M, Carissimo B (2007) Numerical simulations of pollutant dispersion in an idealized urban area, for different meteorological conditions. Boundary-Layer Meteorol 122(2):321–342

Milliez M, Carissimo B (2008) Computational fluid dynamical modelling of concentration fluctuations in an idealized urban area. Boundary-Layer Meteorol 127(2):241–259

Molina MJ, Molina LT (2004) Megacities and atmospheric pollution. J Air Waste Manag Assoc 54(6):644–680

Monin AS, Yaglom AM (1971) Statistical fluid mechanics, vol 1. The MIT Press, Cambridge, U.S.A., 769 pp

Morrison NL, Webster HN (2005) An assessment of turbulence profiles in rural and urban environments using local measurements and numerical weather prediction results. Boundary-Layer Meteorol 115(2):1472–1573

Neophytou MK, Britter RE (2004) Comparison of predictions from the ASUDM (Another Simple Urban Dispersion Model) with results from the DAPPLE tracer field experiment. DAPPLE Cambridge Note 4. http://www.dapple.org.uk

Neumann J (1978) Some observations on the simple exponential function as a Lagrangian velocity correlation function in turbulent diffusion. Atmos Environ 12(10):1965–1968

Pasquill F (1974) Atmospheric Diffusion, 2nd edn. Ellis Horwood Ltd./Wiley, Chichester/New York, 429 pp

Pearson K (1897) Mathematical contributions to the theory of evolution – On a form of spurious correlation which may arise when indices are used in the measurement of organs. Proc Roy Soc Lond 60:489–498

Rappolt T (2001) Field test report: measurements of atmospheric dispersion in the Los Angeles urban environment in summer 2001. Technical Report 1322, Prepared for Simulation Technology Inc., 43 N. Bond St., Bel Air, MD 21014, by Tracer Environmental Science and Technology Inc., 970 Los Vallecitos Boulevard, Suite 100, San Marcos, CA 92069, 33 pp + Data CD

Reed JL (1921) On the correlation between any two functions and its application to the general case of spurious correlations. J Wash Acad Sci 11:449–455

Robins A, Cheng H (2003) Initial dispersion experiments in the EnFlo wind tunnel. DAPPLE EnFlo Note 1. http://www.dapple.org.uk

Rotach MW (1995) Profiles of turbulence statistics in and above an urban canyon. Atmos Environ 29(13):1473–1486

Rotach MW, Vogt R, Bernhofer C, Batchvarova E, Christen A, Clappier A, Feddersen B, Gryning SE, Martucci G, Mayer H, Mitev V, Oke TR, Parlow E, Richner H, Roth M, Roulet YA, Ruffieux D, Salmond JA, Schatzmann M, Voogt JA (2005) BUBBLE—an urban boundary layer meteorology project. Theor Appl Climatol 81(3-4):231–261

Roth M (2000) Review of atmospheric turbulence over cities. Q J Roy Meteorol Soc 126(564):941–990

Stull RB (1988) An introduction to boundary layer meteorology. Kluwer, Dordrecht, 666 pp

Taylor GI (1921) Diffusion by continuous movements. Proc Lond Math Soc 20:196–211

Tennekes H (1979) The exponential Lagrangian correlation function and turbulent diffusion in the inertial subrange. Atmos Environ 13(11):1565–1567

Venkatram A, Upadhyay J, Yuan J, Heumann J, Klewicki J (2002) The development and evaluation of a dispersion model for urban areas. In: Proceedings of the 8th international conference on Harmonization within atmospheric dispersion modeling for regulatory purposes, Sofia, Bulgaria, Demetra Ltd., Akad. G. Bonchov Str., Block 8, 1113, vol 8, pp 320–324

Venkatram A, Isakov V, Pankratz D, Heumann J, Yuan J (2004) The analysis of data from an urban dispersion experiment. Atmos Environ 38(22):3647–3659

Venkatram A, Isakov V, Pankratz D, Yuan J (2005) Relating plume spread to meteorology in urban areas. Atmos Environ 39(2):371–380

Vickers D, Thomas CK, Martin JG, Law B (2009) Self-correlation between assimilation and respiration resulting from flux partitioning of eddy-covariance $CO_2$ fluxes. Agric For Meteorol 149(9):1552–1555

Watson TB, Heiser J, Kalb P, Dietz RN, Wilke R, Wieser R, Vignato G (2006) The New York City urban dispersion program March 2005 field study: tracer methods and results. Technical Report BNL-75592-2006, Brookhaven National Laboratory, P.O. Box 5000, Upton, NY 11973-5000

Yee E, Biltoft CA (2004) Concentration fluctuation measurements in a plume dispersing through a regular array of obstacles. Boundary-Layer Meteorol 111(3):363–415

Yule GU (1910) On the interpretation of correlations between indices or ratios. J Roy Stat Soc Ser A 73:644–647